



## Testing and Comparing the Original Image with the Restored Image that was Obtained by Using the Erosion of the Dilated Image by the AFM Tip

**Ahmed Ahtaiba\***

*Electrical and Electronic Engineering Department, Sirte University, Sirte, Libya*

**\*Corresponding Author:** Ahmed Ahtaiba, Electrical and Electronic Engineering Department, Sirte University, Sirte, Libya.

**Received:** March 05, 2025

**Published:** March 19, 2025

© All rights are reserved by **Ahmed Ahtaiba.**

### Abstract

Atomic force microscopes (AFMs) can measure the surfaces of metals, semiconductors, and insulators. These microscopes can function in various environments, such as vacuum, liquids, or air, and are highly sensitive to atomic forces. AFMs are regarded as extremely high-resolution tools, used for imaging, measuring, manipulating, and probing objects at the micro and nano scales. Unlike other high-resolution microscopes, such as the Scanning Tunneling Microscope (STM), AFMs can examine both conductive and non-conductive materials. In this paper, we present the computer simulation results for morphological deconvolution (dilation and erosion). Using the Matlab peaks function as object and half sphere shaped tip.

**Keywords:** AFM; Erosion; Dilation Image Restoration; AFM Tip; Morphological Deconvolution

### Introduction

Scanning Probe Microscopy (SPM), primarily comprising Atomic Force Microscopy (AFM) and Scanning Tunneling Microscopy (STM), offers three-dimensional topographical images with resolutions that reach, or are near to, the atomic scale. However, while such high-resolution images are crucial for accurate measurements, distortions caused by the AFM tip can become significant when the sample contains features with aspect ratios similar to that of the tip. These distortions result from tip-sample interactions during the imaging process, where the tip scans the surface of the sample. Various techniques can be applied to minimize or eliminate these distortions. In this paper, we employ a dilation operation to simulate the interaction between the object and the AFM tip, followed by an erosion operation between the AFM image (the dilated image) and the AFM tip to restore the image. The simulated AFM tip geometry, represented as a half-sphere, is used for scanning the object, which is modeled using the Matlab peaks function.

### Morphological deconvolution

The operations, erosion, and dilation, are fundamental to morphological image processing: Erosion and dilation are the core operations in the field of morphological image processing [1]. Operations, such as opening and closing, rely on the two primitive operations, erosion and dilation: Techniques like opening and closing depend on the basic operations of erosion and dilation [2]. In this section of the paper, we have used a dilation operation to interact between the simulated object and the simulated AFM tip. An erosion operation has been carried out between the AFM image (the dilated image) and the AFM tip to restore the AFM image: In this part of the paper, we applied a dilation operation to simulate the interaction between the object and the AFM tip. To restore the AFM image, an erosion operation was conducted between the dilated AFM image and the AFM tip [3]. Here, three different geometries of simulated AFM tips (pyramidal, half-sphere, and cone-shaped tip)

have been used for scanning two different simulated objects (the Matlab peaks function): In this study, three different AFM tip geometries (pyramidal, half-sphere, and cone-shaped) were employed to scan two distinct simulated objects using the Matlab peaks function) [4].

**Erosion for binary images**

An erosion operation thins, or shrinks, objects within a binary image, where the fashion and the level of the thinning or shrinking are based on the shape of the particular structuring element used to perform the erosion: Erosion reduces or shrinks objects within a binary image, with the extent and manner of the reduction being determined by the shape of the structuring element applied during the erosion process [5].

Let  $Z$  be the set of real integers.

If  $A$  and  $B$  are sets in  $Z^2$ , then the erosion of  $A$  by  $B$  is determined as

$$A \ominus B = \{z | (B)_z \subseteq A\} \text{ ----- (1)}$$

Where the notation  $\ominus$  represents the erosion and the notation  $A \subseteq B$  represents that  $A$  is a subset of  $B$ .

$(B)_z$  is the translation of a set  $B$  by a point  $z = (z_1, z_2)$  and it is defined as  $(B)_z = \{c | c = b + z, \text{for } b \in B\}$  ----- (2)

In other words, the erosion of set  $A$  by set  $B$  consists of all the positions where the origin of the structuring element does not overlap with any common elements between  $B$  and the background of  $A$  [6]. This erosion process can be represented in the following equivalent form.

$$A \ominus B = \{z | (B)_z \cap A^c = \emptyset\} \text{ ----- (3)}$$

Where  $A^c$  is the complement of  $A$   
 $\emptyset$  is the empty set.

**Dilation for binary images**

Unlike an erosion operation, which thins objects in an image, a dilation operation expands or enlarges objects within the image [7]. The extent and manner of this enlargement depend on the shape of the structuring element used.

If  $A$  and  $B$  are sets in  $Z^2$ , then the dilation of  $A$  by  $B$  is determined as

$$A \oplus B = \{z | (\hat{B})_z \cap A \neq \emptyset\} \text{ ----- (4)}$$

The symbol  $\oplus$  represents the dilation operation, while  $\hat{B}$  refers to the reflection of  $B$  about its origin. A structuring element can be described as a matrix consisting solely of 1's and 0's. This matrix,

which defines the structuring element, can vary in size and shape. The neighborhood is determined by the pixels that hold a value of 1. The fundamental operations of dilation and erosion are not limited to binary images but can also be applied to greyscale images [8].

An example of a dilation is illustrated in Figure 1. Dilation is employed to expand set  $A$  by utilizing the structuring element (set  $B$ ). The dilation process involves reflecting  $B$  about its origin and then shifting this reflection by  $Z$ , so that  $\hat{B}_z$  and  $A$  overlap by at least one element [9]. Dilation of set  $A$  by structuring element  $B$  is shown shaded in Figure 1(c).

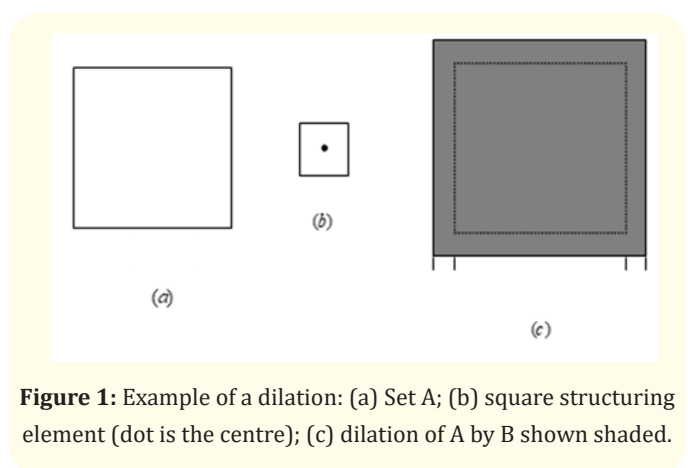


**Figure 1:** Example of a dilation: (a) Set A; (b) square structuring element (dot is the centre); (c) dilation of A by B shown shaded.

Figure 2 illustrates an example of the erosion operation on set  $A$  using a square structuring element  $B$  (with the dot representing the center). The erosion process reduces the size of set  $A$  by applying structuring element  $B$  [10]. The erosion of set  $A$  by set  $B$ , denoted as  $(A \ominus B)$ , consists of all points  $Z$  where the translated version of  $B$  intersects entirely within set  $A$ .

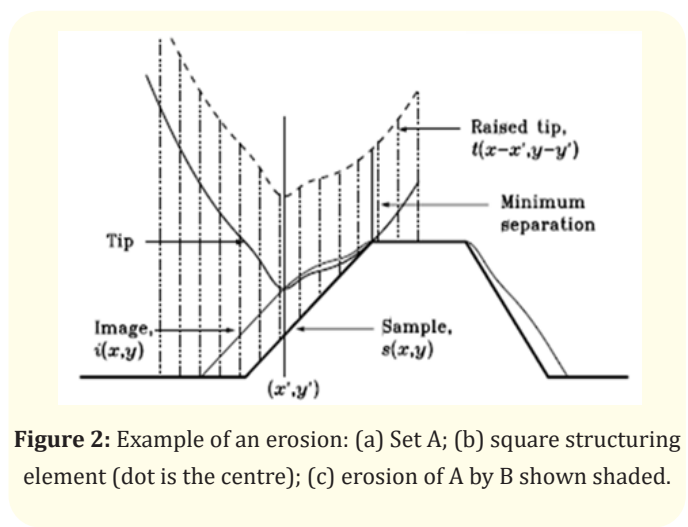


**Figure 2:** Example of an erosion: (a) Set A; (b) square structuring element (dot is the centre); (c) erosion of A by B shown shaded.

**Demonstration that Atomic Force Microscope imaging is equivalent to dilation**

Let  $t(x,y)$  be the function describing the sample’s surface geometry,  $t(x,y)$  be the AFM tip surface, and  $i(x,y)$  the image surface that are each respectively illustrated in Fig..3. When the tip is moved to the point ,  $(x',y')$ , the apex of the tip will mark the height of the image at the point  $(x',y')$  when the tip is in touch with the surface of the sample. That is,

$$i(x',y') = -\min_{(x,y)} [t(x - x', y - y') - s(x, y)] \text{ ----- (5)}$$

Since  $-\min(b) = \max(b)$

Now we make this change of variables

$$x = x' - u \text{ and } y = y' - v$$

After these changes equation (5) becomes

$$i(x',y') = \max_{(u,v)} [s(x' - u, y' - v) - t(-u, -v)] \text{ ----- (6)}$$

$x'^{-}u$  and  $u$  represent the same region since  $x'$  changes from  $x$  to  $x'$ . This leads us to use the fact that is,

$$\max_{x'-u} = \max_u$$

Now a new function is defined

$$p(x, y) = -t(-x, -y) \text{ ----- (7)}$$

Where  $p(x, y)$  is the reflection of the tip through the origin.

By this new function equation (6) becomes

$$i(x, y) = \max_{(u,v)} [s(x - u, y - v) + p(u, v)] \text{ ----- (8)}$$

It is evident that equation (8) means

$$I = S \oplus P \text{ ----- (9)}$$

Where  $I$  is the image surface,  $S$  the sample, and  $P$  is the reflection of the tip.

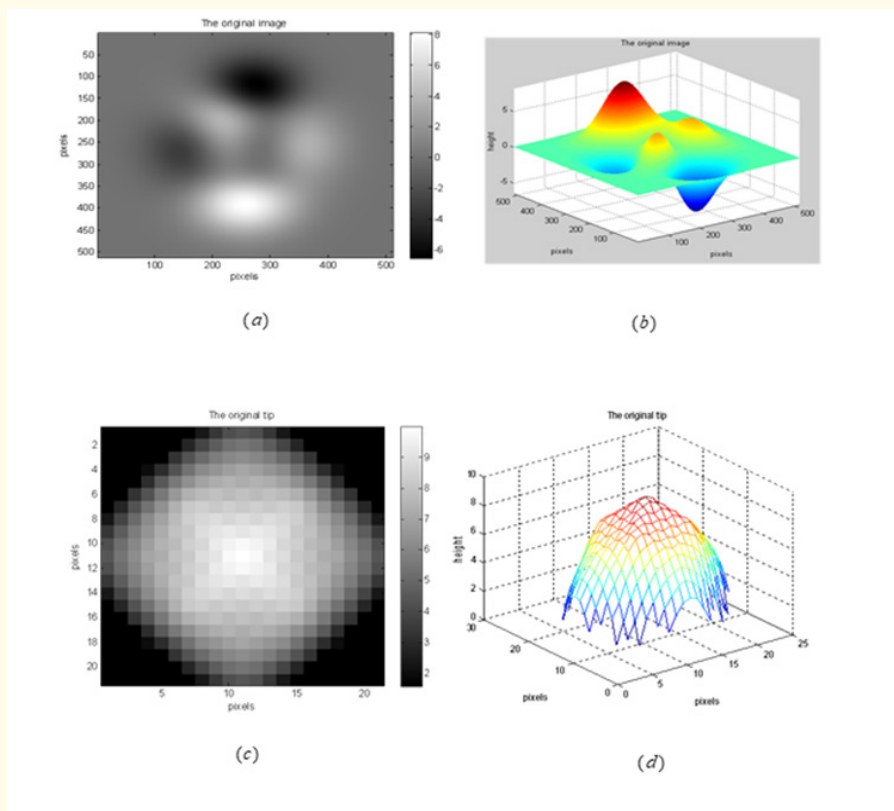


**Figure 3:** The conventional model for imaging.

**Computer simulation results**

In this paper, the results of computer simulations for morphological deconvolution (dilation and erosion) are presented. This method of morphological deconvolution has been implemented by utilizing a dilation operation between the simulated original atomic force microscope (AFM) tip and the object for AFM imaging. An erosion operation has been applied between the simulated original AFM tip and the dilated image, which corresponds to the raw AFM image, for the purpose of restoring the AFM image. The computer simulations were conducted to test and compare the original image with the restored image obtained through the erosion of the dilated image by the tip.

**Simulation results using the Matlab peaks function as an object and a half sphere-shaped tip**

Figure 4 presents the simulation results obtained using a half-sphere-shaped tip and a sample represented by the Matlab peaks function. In this context, the AFM image can be conceptualized as a dilation of the sample influenced by the geometry of the original AFM tip, which, in this instance, is the half-sphere-shaped tip

$$I_s = S \oplus P \text{----- (10)}$$

Where  $I_s$  is the AFM image that is produced by a dilation operation between the object (the peaks function) and the original AFM tip (a half sphere shaped tip).

$S$  is the original image of the sample, here the sample (object) is represented by the peaks function.

$P$  is the original tip shape, that is a half sphere-shaped tip.

If the genuine surface topography and the sample are known, then by an erosion operation the reconstructed image is given by

$$S_r = I_s \ominus P \text{----- (11)}$$

Here,  $S_r$  denotes the reconstructed image obtained through an erosion process between the AFM image (the dilated image) and the original AFM tip, which is shaped like a half-sphere. This section employs a computer simulation designed to construct both the original AFM tip and the sample (the original image). The AFM tip is modeled as a half-sphere, while the sample is represented by the peaks function, as illustrated in Figures 4 (a), (b), (c), and (d). Specifically, Figures 4 (a) and (b) depict the 2D and 3D representations of the original image, respectively, while Figures 4 (c) and (d) showcase the 2D and 3D representations of the AFM tip.

The AFM image is generated through a dilation operation between the sample, represented by the peaks function, and the half-sphere-shaped AFM tip. The resulting 2D and 3D dilated images are shown in Figures 4 (e) and (f), respectively. Finally, the sample is reconstructed using an erosion operation applied between the sample (peaks) and the AFM tip (half-sphere-shaped tip). The reconstructed image is illustrated in Figures 4 (g) and (h), representing the 2D and 3D reconstructed images, respectively.

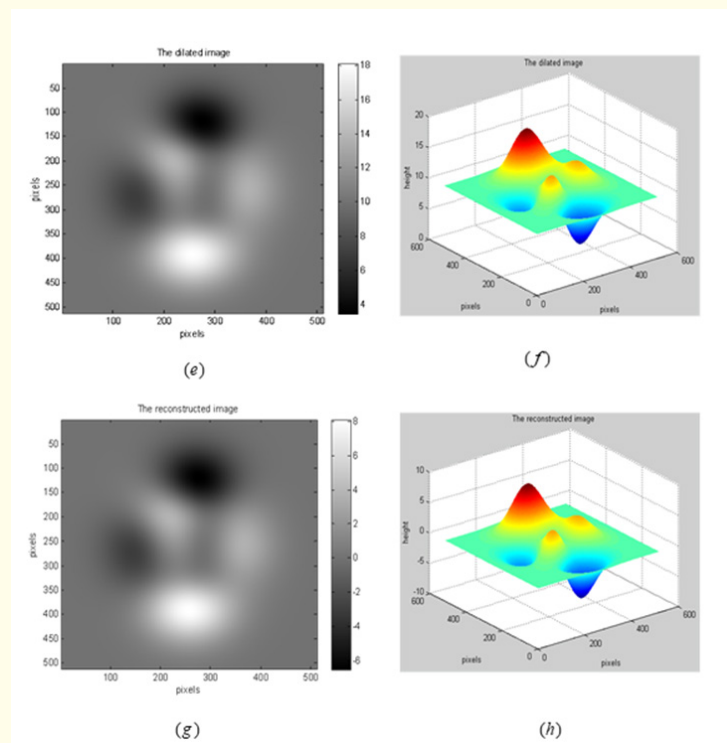


**Figure 4:** Illustrates the simulation results utilizing the computer-simulated peaks function as the object along with a half-sphere-shaped tip. The components are detailed as follows: (a) the 2D original image (peaks); (b) the 3D original image; (c) the 2D representation of the half-sphere-shaped tip; (d) the 3D representation of the half-sphere-shaped tip; (e) the 2D AFM image (dilated image); (f) the 3D AFM image (dilated image); (g) the 2D reconstructed image, which results from the erosion operation between the AFM tip and the AFM image (dilated image); and (h) the 3D reconstructed image.

Figures 5(a) and (b) depict the error image between the original image (peaks), shown in Figure 4 (a), and the restored image, illustrated in Figure 4 (g), in both two-dimensional and three-dimensional forms, respectively.

The error calculations comparing the original image to the restored image, based on simulation results using the Matlab peaks function as the object and a half-sphere-shaped tip, are detailed in Table 1. The statistics include a mean error value of 1.855 nm, a

standard deviation of 1.402 nm, a minimum error of 0 nm, a maximum error of 10.011 nm, and a root mean square error of 1.855 nm.

Table 1 presents the error calculations between the original image and the restored image based on simulation results that utilize the Matlab peaks function as the object and a half-sphere-shaped tip.

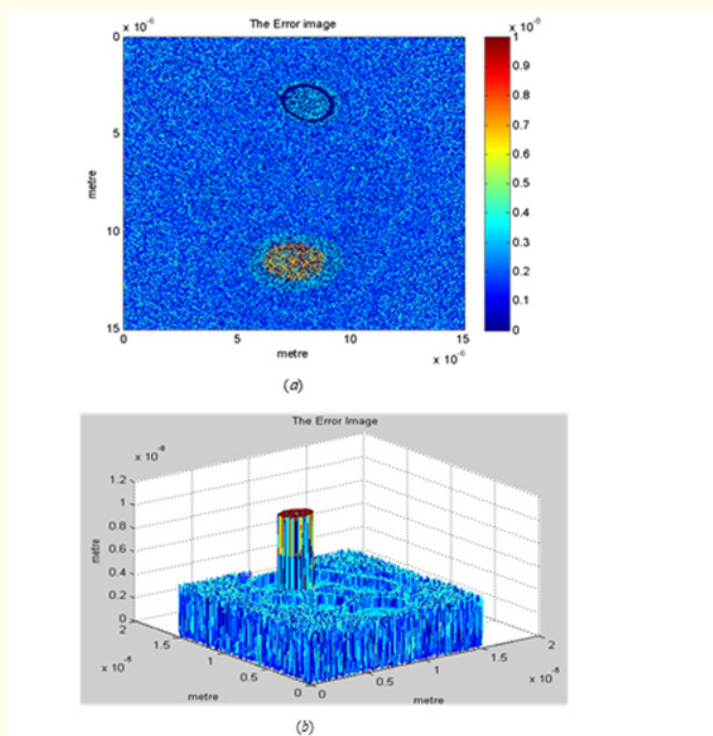


**Figure 5:** Shows the error image between the original image (peaks) presented in Figure 4 (a) and the restored image illustrated in Figure 4 (g). Specifically, (a) displays the 2D error image, while (b) shows the 3D error image.

Mean of error [nm]	Standard deviation of error [nm]	Minimum error [nm]	Maximum error [nm]	RMSE [nm]
1.855	1.402	0	10.011	1.855

**Table 1:** Shows the error calculations between the original image and the restored image.

### Conclusion

Several algorithms can be employed to reconstruct AFM images, and a variety of these techniques have been reviewed and implemented in this study. This paper has examined the theory behind morphological deconvolution techniques. Computer simulations were conducted using the Matlab peaks function and a simulated AFM tip geometry, specifically a half-sphere-shaped tip. As illustrated in Table 1, the restoration of the object is improved when utilizing the half-sphere-shaped tip in the computer simulation. The error calculations comparing the original image to the re-

stored image are also presented in Table 1. The results indicate that the best restoration of the Matlab peaks function object is achieved with the use of the half-sphere-shaped tip.

### Contribution of Individual Authors to the Creation of a scientific Article

The authors equally contributed in the present research, at all stages from the formulation of the problem to the final findings and solution.

### Sources of Funding for Research

No funding was received for conducting this study.

### Conflict of Interest

The authors have no conflicts of interest to declare that are relevant to the content of this article.

### Bibliography

1. A Ahtaiba. "The Improvement in The AFM Image after Applying a Lucy- Richardson Deconvolution Algorithm using a New Technique for Estimating the AFM Tip Shape from the Square Sample". *Journal of Wseas Transactions on Signal Processing* 19 (2023): 103-107.
2. Y Andrew and K Ludger. "Aspects of Scanning Force Microscope Probes and their Effects on Dimensional Measurement". *Applied Physics* 41 (2008): 1-46.
3. K Angelika., *et al.* "AFM - tip- integrated amperometric microbiosensors: High- resolution imaging of membrane transport". *Angewandte Chemie International Edition* 44 (2005): 3419-3422.
4. J Schneir, *et al.* "In fourth workshop on industrial applications of scanning probe microscopy". NIST Gaithersburg, MD, USA (1997): 30-31.
5. H Yasuhiko., *et al.* "Estimation of three dimensional Atomic Force Microscope tip shape from Atomic Force Microscope image for accurate measurement". *Japanese Journal of Applied Physics* 47.7 (2008): 6186-6189.
6. N Masao., *et al.* "Critical dimension measurement in nanometer scale by using Scanning Probe Microscopy". *Japanese Journal of Applied Physics* 35 (1996): 4166-4177.
7. N Masao., *et al.* "Metrology of Atomic Force Microscopy for Si nano-structures". *Japanese Journal of Applied Physics* 34 (1995): 3382-3387.
8. T Wenbing., *et al.* *IEEE Transactions on Systems* 38.5 (2008): 96-99.
9. M Bertero and P Boccacci. "Image restoration methods for the large binocular telescope". *Astronomy and Astrophysics Supplement Series* 147.2 (2000): 323-333.
10. PJ Verveer, *et al.* "A comparison of image restoration approaches applied to three-dimensional confocal and wide-field fluorescence microscopy". *Journal of Microscopy* 193.1 (1999): 50-61.